




# Current and Future Applications of Fluorescence Guidance in Orthopaedic Surgery

Samuel S. Streeter<sup>1</sup>  · Kendra A. Hebert<sup>1</sup> · Logan M. Bateman<sup>1,2</sup> · Gabrielle S. Ray<sup>2,3</sup> · Ryan E. Dean<sup>2,3</sup> · Kurt T. Geffken<sup>2,3</sup> · Corey T. Resnick<sup>2,3</sup> · Daniel C. Austin<sup>2,3</sup> · John-Erik Bell<sup>2,3</sup> · Michael B. Sparks<sup>2,3</sup> · Summer L. Gibbs<sup>4</sup> · Kimberley S. Samkoe<sup>1</sup> · I. Leah Gitajn<sup>2,3</sup> · Jonathan Thomas Elliott<sup>1,2,3,5</sup> · Eric R. Henderson<sup>1,2,3,5</sup>

Received: 18 July 2022 / Revised: 1 November 2022 / Accepted: 16 November 2022 / Published online: 29 November 2022  
© The Author(s), under exclusive licence to World Molecular Imaging Society 2022

## Abstract

Fluorescence-guided surgery (FGS) is an evolving field that seeks to identify important anatomic structures or physiologic phenomena with helpful relevance to the execution of surgical procedures. Fluorescence labeling occurs generally via the administration of fluorescent reporters that may be molecularly targeted, enzyme-activated, or untargeted, vascular probes. Fluorescence guidance has substantially changed care strategies in numerous surgical fields; however, investigation and adoption in orthopaedic surgery have lagged. FGS shows the potential for improving patient care in orthopaedics via several applications including disease diagnosis, perfusion-based tissue healing capacity assessment, infection/tumor eradication, and anatomic structure identification. This review highlights current and future applications of fluorescence guidance in orthopaedics and identifies key challenges to translation and potential solutions.

**Key words** Fluorescence-guided surgery · Indocyanine green imaging · Meniscus tear · Necrotizing soft tissue infection · Nerve imaging · Tissue-simulating phantoms · Tumor imaging

## Introduction

Surgery and other invasive medical procedures are ultimately deemed acceptable based on the risk-to-benefit ratio. In the ideal embodiment, an invasive procedure will accomplish its goal—tumor removal, vascular bypass, etc.—with absolute effectiveness and efficiency and with the least possible harm to normal structures. Radiological imaging has revolutionized what is possible from a procedural standpoint, enabling

non-invasive anatomical guidance to enhance the accuracy and safety of medical procedures.

Molecular imaging has added another dimension to existing technologies, enabling the identification of *physiological* phenomena along with the anatomy under scrutiny. Molecular imaging involves the visualization, characterization, and measurement of microscopic biochemical phenomena. The field spans a wide range of modalities, including positron emission tomography (PET), single photon emission computed tomography (SPECT), computed tomography (CT), magnetic resonance imaging (MRI), ultrasound (US), and optical imaging [1]. Each modality offers strengths and weaknesses, mainly tied to human safety and efficacy for visualizing anatomical structures, tissues, and pathologies, but cost and ease-of-use are also key factors for clinical translation. In the context of surgical guidance, imaging and visualization are ideally real-time with a field of view that matches the surgeon's view of the operative field. A well-known downside of optical imaging in general is limited depth penetration in tissue (cm or less). However, for guidance during surgical procedures where target tissues are (nearly) exposed, optical imaging has the potential to provide valuable molecular sensing [2]. Relative to other

---

✉ Samuel S. Streeter  
Samuel.S.Streeter.TH@Dartmouth.edu

<sup>1</sup> Thayer School of Engineering, Dartmouth College, Hanover, NH 03755, USA

<sup>2</sup> Department of Orthopaedics, Dartmouth Health, Lebanon, NH 03756, USA

<sup>3</sup> Geisel School of Medicine, Dartmouth College, Hanover, NH 03755, USA

<sup>4</sup> Oregon Health & Science University, Portland, OR 97239, USA

<sup>5</sup> Dartmouth Cancer Center, Dartmouth Health, Lebanon, NH 03756, USA

modalities, optical imaging is safe (*i.e.*, non-ionizing), rapid (*i.e.*, capable of video rate), adaptable in form factor and field of view, and cost-effective compared to many conventional medical imaging techniques.

Fluorescence-guided surgery (FGS) is a nascent, optical technique that seeks to improve the recognition of anatomical structures and disease processes through machine-assisted, visual identification using fluorescent probes [2]. Information gleaned from fluorescence guidance ideally facilitates improved surgeon decision-making by enhancing delineation of important anatomic or physiologic processes that will ultimately improve patient outcomes. Clinical indications for FGS are far-reaching [2]. Examples include the assessment of corneal or vessel abnormalities in the eye (ophthalmology), assessment of vascular perfusion in free-flap reconstruction (plastic surgery), and evaluation of blood flow and renal flow in the kidneys (urology) [3]. FGS offers clinical value in several types of surgical oncology, including the treatment of ovarian, breast, and lung cancers, [4], and is nearing clinical translation for the treatment of gastrointestinal and head and neck cancers [5]. The most impactful FGS application to date is perhaps in neurosurgery, where oral administration of the fluorophore 5-aminolevulinic acid is known to provide high sensitivity, specificity, and positive predictive value for identifying malignant glioma tumor tissue [6].

While FGS applications have disseminated quickly to many surgical specialties, investigation and adoption in orthopaedic surgery have lagged [7]. The purpose of this review is to highlight early investigations into FGS applications in orthopaedic surgery and identify areas ripe for future exploration. To date, orthopaedic-specific FGS spans three general applications (Fig. 1): (1) infection management [8, 9]; (2) perfusion-based assessment of tissue healing capacity [10, 11] and joint repairs [12, 13]; and (3) tissue identification, most notably for connective-tissue cancer treatment [14–18] and nerve imaging to mitigate iatrogenic injuries during surgeries [19–22]. The following sections of this review are dedicated to each of these three broad clinical applications with specific examples from ongoing research at a tertiary care medical center. Finally, key challenges to translation and potential solutions are highlighted, including new fluorophore evaluation and lead agent selection, tissue-simulating fluorescent phantoms, and fluorophore and imager evaluation.

## Tissue Infection Management

### Diagnostic Assessment of Soft Tissue Infection

The detection and treatment of infection is a priority of the World Molecular Imaging Society (WMIS) through the

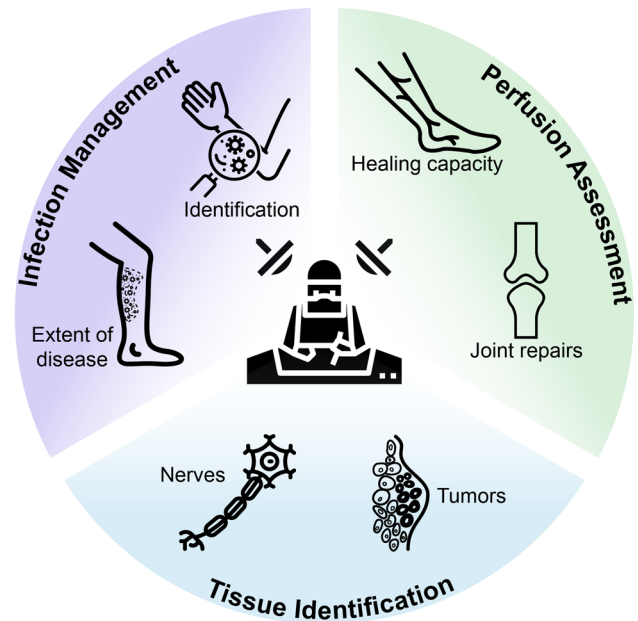


**Fig. 1** Overview of the three general applications of fluorescence guidance in orthopaedic surgery discussed in this review article: tissue infection management, perfusion-based assessment of tissue healing capacity and joint repairs, and nerve and tumor tissue identification.

Imaging of Infections Interest Group [23]. To date, most research in this area is accomplished with nuclear imaging modalities (*e.g.*, PET or SPECT) and functionalized radiotracers that preferentially bind to pathogens or therapeutic agents [24]. For example, in the context of orthopaedics, recent work by Gordon et al. demonstrated that drug delivery to orthopaedic implant-associated bone infections was lower than previously thought using dynamic PET imaging, suggesting higher doses are needed for efficacious treatment of implant infections [25]. Others have used fluorescence imaging to detect bacterial biofilms on implants, such as Schoenmakers et al., who recently conjugated an antibiotic to the near-infrared (NIR) fluorophore IRDye800CW, enabling real-time detection and treatment of prosthetic joint infections [26]. The detection of soft tissue infections has historically relied on MRI, X-ray imaging, US, and nuclear imaging [27], but optical fluorescence imaging is an attractive alternative for non-ionizing, real-time, cost-effective detection.

Soft tissue infection imaging using fluorescence relies primarily on targeted agents [8, 9]. However, an alternative approach is to leverage vascular changes in the form of infection-induced thrombi in affected tissues [28] using perfusion-based fluorescence imaging. An exemplar application is perfusion imaging for the detection and surgical debridement of necrotizing fasciitis (NF). NF is a type of rapidly progressing soft tissue infection with a cumulative

mortality rate of 34% [29, 30]. Clinical consensus guidelines on the evaluation and treatment of NF involve prompt surgical consultation—typically leading to emergent and aggressive surgical debridement of affected tissues—and broad antibiotic treatment due to the possibility of polymicrobial etiology [31]. Current diagnostic methods have low specificity as patients often present with a nonspecific constellation of symptoms [30, 32], and infected tissues often appear unremarkable (Fig. 2a). Widespread, superficial thrombosis is a nearly universal finding on histological analysis of NF-affected tissues mediated via a pro-inflammatory effect on the microcirculation by causative bacteria [29, 33]. The field of FGS has largely focused on perfusion assessment using indocyanine green (ICG) [34]. Fluorescence imaging using ICG allows for rapid and repeatable examinations of perfusion changes in real-time and is Food and Drug Administration (FDA)-approved with several commercial devices successfully and reliably used in different surgical subspecialties. A novel application of ICG-based perfusion imaging is its use as a diagnostic modality in patients with suspected NF to compare NF-affected tissues to unaffected tissues given the underlying vascular thrombosis.

Patients deemed clinically to be at risk of NF were given a weight-based dose of ICG (0.2 mg/kg), and fluorescence kinetic signatures were measured from suspicious tissue regions and adjacent, normal-appearing tissues (NCT04839302). The institutional review board (IRB)-approved protocol for this pilot study involved enrolling 15 patients in total. Images were recorded using the SPY Elite imaging system (Stryker-Novadaq, Kalamazoo, MI)

at video rate for 10 s prior to injection of ICG to establish a baseline. ICG was then administered intravenously, and the recording continued for four min. Patients were then taken to the operating room for debridement and confirmed as NF-positive or NF-negative based on histopathologic diagnosis of tissue specimens. Early data from this pilot study demonstrate that distinct ICG signal voids occur in NF-positive tissues (Fig. 2b). ICG kinetic profiles were parameterized to create four kinetic features: max intensity (Imax), time-to-peak (TTP), ingress slope (IS), and egress slope (ES) (Fig. 2c). NF-positive tissues exhibit peak fluorescence intensities < 100 a.u. versus > 250 a.u. for NF-negative tissues (Fig. 2e). ES assesses the vascular dynamics of fluorescence wash-out over time. ES values of  $\sim -1.5$  were observed in NF-negative tissues versus  $\sim -0.1$  in NF-positive tissues (Fig. 2h).

Initial results demonstrate significantly lower fluorescence in tissues affected by NF compared with tissues unaffected by NF. NF-unaffected tissues appear to exhibit a hyperemic response. Vascular dynamics based on ES suggest slow wash-out due to venous congestion or leakiness in NF-affected tissues. Results also suggest that ICG fluorescence imaging can be used as a diagnostic tool in management of NF. Future work may involve: (1) identification of ICG fluorescence-to-histopathology correlates in NF-affected tissues that indicate bacterial burden and delineate appropriate surgical debridement; (2) exploration of additional fluorophores (*e.g.*, fluorescein, which has an emission peak in the visible range) that could provide perfusion-based, direct visual guidance on the

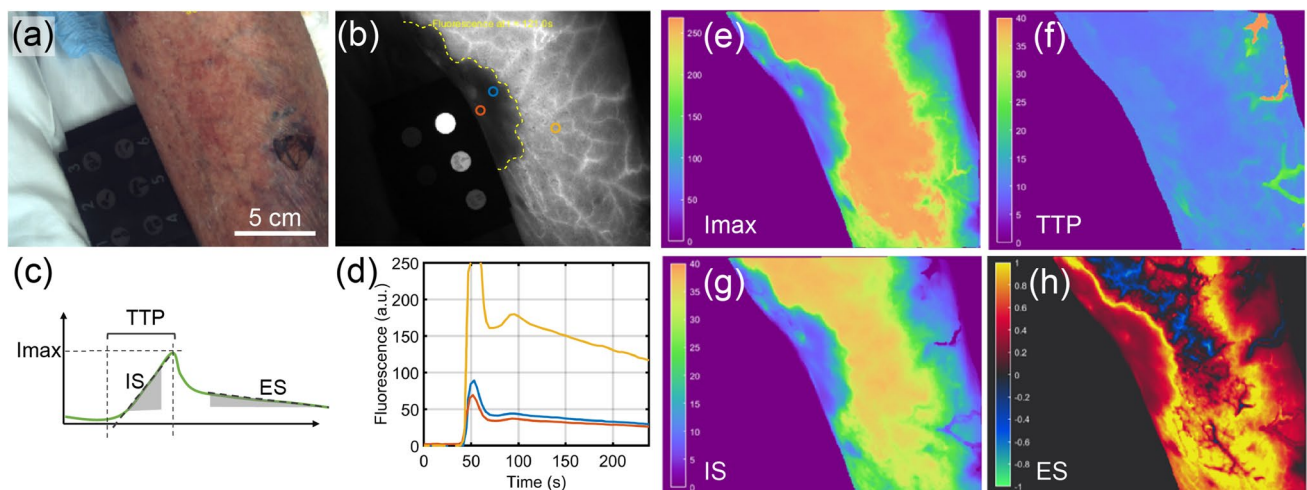


**Fig. 2** Representative patient presenting with confirmed necrotizing fasciitis (NF) in the lower leg. **a** White light color image shows minimal contrast to disease extent. **b** Wide-field ICG image at two-min post-injection reveals approximate extent of disease (yellow dashed line) with disease represented by ICG signal void; quantitative fluorescence standard (QUEL Imaging, White River Junction, VT) is shown on left; regions of interest depict deep NF-affected tissue (red),

near-boarder NF-affected tissue (blue), and unaffected tissue (yellow). **c** Time-resolved fluorescence kinetic curve parameterization yields four features: max intensity (Imax), time-to-peak (TTP), ingress slope (IS), and egress slope (ES). **d** Kinetic curves extracted from the three regions of interest defined in (B). **e** Imax parameter map. **f** TTP parameter map. **g** IS parameter map. **h** ES parameter map. Scale bar in **a** also applies to **b, e–h**.

surgical field; and (3) development of surgical imagers with real-time display of interpretive data on the surgical field (*e.g.*, via a raster-scanning laser). Finally, the use of fluorescent signal kinetic signatures could extend beyond NF for the characterization of other types of soft tissue infections.

## Tissue Perfusion and Tissue Healing Capacity Assessment

### Meniscal Healing Capacity Assessment

Recent advancements in arthroscopic technology have created opportunities for minimally invasive assessment of soft tissue vascularity. Meniscal tears are one of the most common injuries to the knee with an incidence rate of 12–14% and pose significant long-term morbidity [35]. Treatment options range from non-operative, in the form of physical therapy or injections, to operative, involving resection or repair [36, 37]. Regardless of management options, a high percentage of patients develop post-traumatic arthritis [38].

Meniscal cartilage is unique in that approximately two-thirds of it is hypovascular, with the outer, low-perfusion regions possessing minimal healing potential [39, 40]. Furthermore, the delineation of these vascular and hypovascular regions is not defined visually, making the intraoperative decision of resection versus repair difficult and subjective [41, 42]. Providing an objective measure of vascularity would improve surgical decision-making, allowing for repair of meniscal tears when appropriate and indicating when partial meniscectomy is indicated. This would ultimately result in improved patient outcomes [37]. Secondly, better decision-making for meniscal injury management could delay the onset of osteoarthritis and thereby decrease the demand for total knee arthroplasty [36].

This clinical problem prompted initiation of a pilot study to determine the efficacy of ICG-based fluorescence arthroscopy in evaluating meniscal blood supply (NCT05072717). The IRB-approved protocol for the study involved enrolling 30 patients in total. Eligible patients received a weight-based dose of ICG (0.2 mg/kg) prior to image capture using a fluorescence arthroscope (Image1 S 4U Rubina OPAL 1, Karl Storz, Tuttlingen, Germany). Imaging was performed at video rate for 10 s prior to injection and for four min following injection. The surgeon then examined various structures of the knee for perfusion assessment including the meniscal tear, healthy portions of the meniscus, and the synovium of the knee. Adjacent structures, such as the anterior cruciate ligament and bony cartilage, were also examined. This work differed from perfusion studies in an open surgical field, because using a fluorescence

arthroscope presented several unique challenges, including balancing arthroscopic pump pressure with the visualization of ICG, mobile position of the scope during agent wash-in and wash-out, and adjusting imaging acquisition settings to optimize fluorescence visualization. Preliminary results from this pilot study are promising with images demonstrating penetration of ICG into various intracapsular structures (Fig. 3). Figure 3a depicts ICG signal intensity within the microvasculature of a representative knee joint, demonstrating the potential for visualization of small caliber vessels with high resolution. Figure 3b depicts a second case where ICG clearly permeates from the hypervascular synovium through the meniscal capsular junction and into the red-red zone of the meniscus.

Additional study cases will allow for refinement and standardization of the imaging procedure. If proven successful, this technology would allow orthopaedic surgeons to make decisions regarding resection versus repair based on objective data rather than conjecture. It is theorized that making data-driven decisions would also translate to improved patient outcomes, fewer repeat surgeries, and delayed progression of osteoarthritis secondary to meniscal loss. This ultimately could prolong longevity of native knees, decrease the case burden of severe osteoarthritis on our healthcare system, and decrease healthcare costs.

### Shoulder Surgery

Shoulder arthroplasty is a common operation performed for glenohumeral joint arthritis with strong clinical success [43]. Of the four muscles comprising the rotator cuff, the subscapularis is of particular concern in shoulder arthroplasty due the common use of an anterior surgical approach, which requires temporary removal—“takedown”—of the subscapularis tendon insertion. Three common subscapularis takedown techniques exist with no

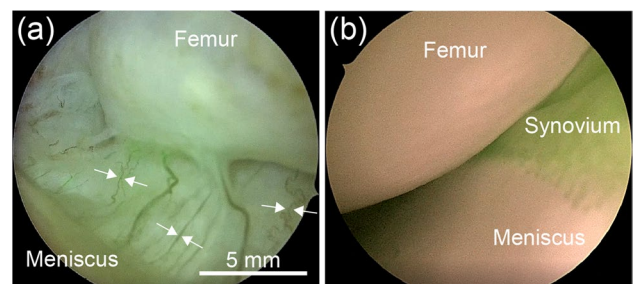


**Fig. 3** Two representative knee joints imaged using the Image1 S RU Rubina OPAL 1 arthroscope (Karl Storz, Tuttlingen, Germany). **a** ICG signal intensity enables high-contrast visualization of joint microvascular (white arrows). **b** ICG signal visualizes well-perfused synovial tissue and highlights regions of low and potentially jeopardized perfusion corresponding to fluorescence signal voids. The 5-mm scale bar in **a** also applies to **b**.

academic consensus about which is superior [44]. These techniques are the following: (1) lesser tuberosity osteotomy; (2) subscapularis peel; and (3) subscapularis tenotomy. Each technique requires repair, which is crucial for proper shoulder force coupling to keep the humeral implant centered on the glenoid [45]. Due to the negative impact on patients with subscapularis failure, there is interest in identifying the takedown technique with the best outcomes.

We undertook a pilot study of patients undergoing shoulder arthroplasty via the deltopectoral approach to determine the feasibility of using dynamic, contrast-enhanced fluorescence imaging to measure tendon perfusion (NCT05179941). The IRB-approved protocol for this study involved enrolling 10 patients total. Prior to fluorophore injection, video rate imaging was performed for 20 s for a baseline measurement using the SPY Elite imaging system. A weight-based dose of ICG (0.1 mg/kg) was then injected intravenously, and imaging continued for four min. The shoulder arthroplasty proceeded, utilizing a subscapularis peel or tenotomy, with repair following arthroplasty. Post-repair fluorescence images were acquired and compared to initial images to evaluate tendon perfusion.

Preliminary results indicate pre-procedure peak fluorescence signals (mean  $\pm$  one standard deviation of  $119 \pm 68$  a.u.) are significantly higher than post-procedure peak fluorescence signals ( $58 \pm 27$  a.u.). The average percent change in peak signal intensity between pre- and post-procedure images was  $-40 \pm 40\%$  (Fig. 4). Ongoing work involves correlating these data with clinical outcomes, particularly subscapularis failure.

## Effect of Cable Cerclage on Femoral Bone Perfusion

Healing throughout the body is dependent on blood supply to provide adequate nutrients, oxygenation, and signaling molecules to stimulate, direct, and maintain the healing response [46, 47]. Many studies show that increased disruption to the vascular supply of bone, whether from trauma itself or surgical technique, is a major factor in long-term complications. Maintaining sufficient blood supply is thus vitally important and is recognized as one of the four core tenants of the AO's principles to management of fractures (*Arbeitsgemeinschaft für Osteosynthesefragen*, commonly referred to as AO, is German for “working group for bone fusion issues”) [48].

One common fixation strategy in orthopaedic surgery involves the use of cerclage wires or cables [49, 50]. While an effective tool, cerclage wires place a large force focused through a small surface area of bone, which can effectively crush the periosteum against the cortex. The theory of “strangulation of blood supply” by cerclage wires has been previously investigated using various techniques from cadaveric models to live rabbits [51]. Karakoyun et al. utilized scintigraphy to evaluate blood perfusion around the femoral cortex with and without cable cerclage in a rabbit model and showed significantly decreased blood flow after intervention [52].

Measuring blood flow to bone is nontrivial, usually relying on gestalt perception to sense what is considered “healthy bleeding bone” while in the operating room [11]. ICG-based perfusion imaging for assessing blood flow to bone has been translated from a porcine model into human

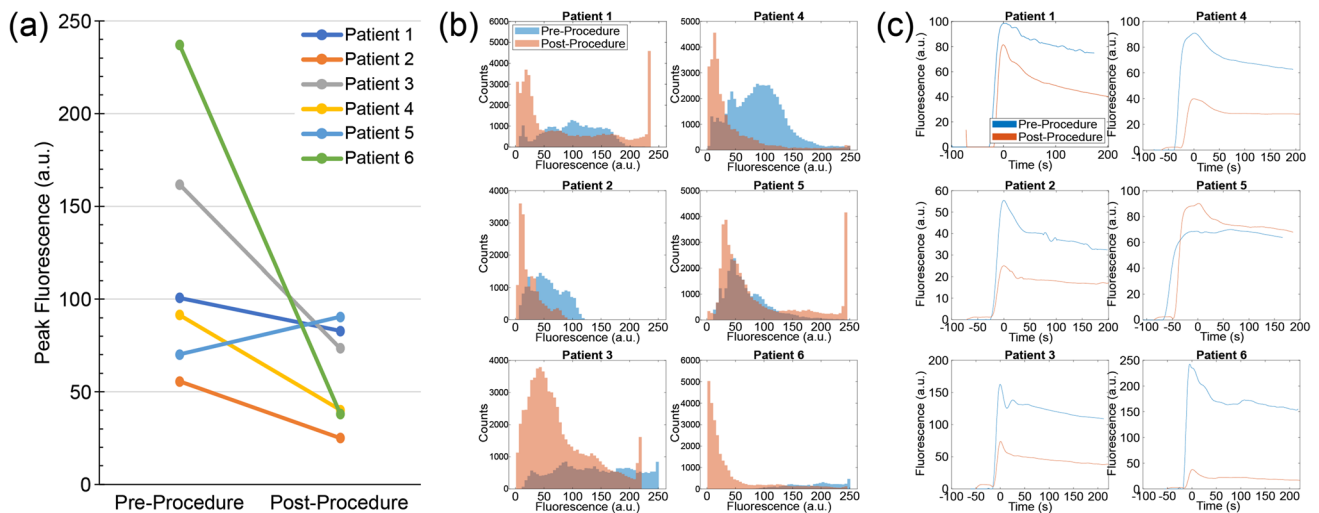


**Fig. 4** Preliminary data of shoulder arthroplasty tendon perfusion assessment in six patients using dynamic, contrast-enhanced ICG imaging. **a** The peak fluorescence intensity pre- and post-procedure for each of six study patients. **b** Distribution of fluorescence intensi-

ties extracted from a region of interest delineating the exposed subscapularis tendon, before and after the procedure. **c** Mean region of interest fluorescence intensity curves for each patient during ICG wash-in and wash-out, before and after the procedure.

patients in two large, federally funded clinical trials [53], and to date, has demonstrated reliable and reproducible data and efficacy.

We initiated a preclinical pilot study to evaluate the effect of femoral cerclage wires on femoral bone perfusion using a rabbit model. It was hypothesized that there would be a significant decrease in flow to areas bounded by cerclage, which would worsen in the setting of more wires/less space between wires. Two perfusion imaging techniques were used in the study: (1) fluorescence imaging via peripheral injection of a weight-based dose of ICG (0.1 mg/kg/injection) with video rate imaging of the exposed femur using the SPY Elite system; and (2) as the gold-standard technique, a weight-based dose of fluorescent microspheres ( $1.5 \times 10^6$  beads/kg) followed by cryomicrotome imaging to create a three-dimensional perfusion map of the femur [54]. For the ICG imaging, baseline perfusion was measured at video rate for 20 s prior to ICG injection and for six min post-injection. Two cerclage wires were passed around the femoral shaft, and imaging was repeated. Two additional cerclage wires were then placed between the first two for a total of four cerclage wires, and imaging was repeated a third time. The preclinical pilot study involved imaging 15 rabbits total.

ICG fluorescence imaging provides quantitative information about how much the cerclage wires decrease blood flow to the bone relative to baseline. Preclinical study data analysis is ongoing. If significant decreases in blood flow are measured, such findings will lead to future studies in this area and possibly changes in fracture management techniques and fixation devices to avoid circumferentially restricting periosteal blood supply, ultimately reducing the occurrence of long-term complications associated with the use of cerclage wires in orthopaedic surgery.

## Tissue Identification

### Connective Tissue Oncological Indications

In general, tissues scrutinized by orthopaedic surgeons arise from the middle germ layer, called the mesoderm. These mesoderm-derived tissues (*i.e.*, bone, muscle, fat, and peripheral nerve) are broadly termed “connective tissues,” and may give rise to benign and malignant neoplasms. Benign connective tissue neoplasms are considered indolent, intermediate, or aggressive; connective tissue-derived cancers are called sarcomas. Our team has explored fluorescence guidance for both benign connective-tissue tumors and sarcomas.

Most benign connective tissue tumors are indolent and require no intervention. Benign-aggressive bone tumors (*e.g.*, giant cell tumor of bone, aneurysmal bone cyst, and chondroblastoma) will continue to grow and result in patient

morbidity; these tumors require intervention. The most common complication following surgical management of benign-aggressive bone lesions is local tumor recurrence, attributed to incomplete tumor removal [55, 56]. To address local recurrence, we undertook a first-in-human trial of “second window” ICG perfusion imaging using the SPY Elite system for benign-aggressive bone lesions requiring intral-lesional removal (NCT05075889). The protocol entailed systemic administration of a weight-based dose of ICG (1.9 mg/kg for adults aged  $\geq 18$  years; 0.5 mg/kg for individuals aged 12–17 years) followed by surgical resection and snapshot imaging 24 h post-injection with the SPY Elite system. A total of 10 patients were enrolled in this IRB-approved trial. Early results indicate useful tumor-to-background contrast (Fig. 5). Additional benign neoplasms with a high rate of local recurrence for which FGS may prove valuable include atypical cartilaginous tumors, tenosynovial giant cell tumor, desmoid tumor (also called fibromatosis), osteoblastoma, and chondromyxoid fibroma.

Sarcomas are classified generally as bone or soft tissue sarcomas (STS). STSs are more than twice as common [57], are mostly resistant to chemotherapy, and show modest responses to radiation; complete surgical excision is therefore the mainstay of curative treatment. Surgical excision of sarcomas occurs ideally with a margin of normal, non-cancerous tissue surrounding the tumor, termed a wide local excision (WLE). Current methods to evaluate WLE margins require several hours to days of pathological processing and analysis. Specimen margins are classified as “negative,” indicating no tumor present at the cut surfaces (*i.e.*, a successful WLE), or a “positive” margin, where tumor is present on one or more surfaces of a resection (*i.e.*, a failed WLE). Real-time knowledge of WLE margin status would be highly valuable to achieve a successful surgical outcome, but no technology is currently available for this purpose.

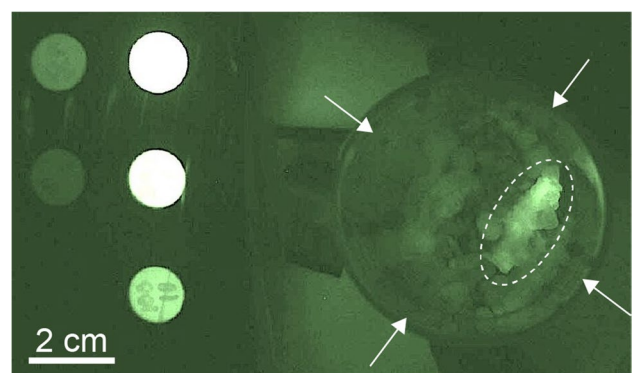


**Fig. 5** Resected (*i.e.*, *ex vivo*) benign-aggressive bone lesion tissue (white dashed line) exhibits increased ICG fluorescence relative to healthy resected tissues (white arrows). Quantitative fluorescence standard is shown on the left (QUEL Imaging, White River Junction, VT). Surgery and imaging performed 24 h post-injection.

Surgical management of sarcomas remains largely unchanged over the last three decades. Currently, surgeons rely on radiologic imaging, anatomical landmarks, and visual and tactile input to guide excision. These management techniques result in inconsistent margin thickness, with the unnecessary removal of vital tissues or incomplete cancer excision, both resulting in poorer patient outcomes. The largest series by Pisters et al., published in 1996, found that positive margins occurred in 23% of sarcoma surgeries, leading to cancer recurrence and reduced survival [58]; no improvements in outcomes have been reported since that time.

Our oncological FGS research has focused mainly on fluorescence-based methods of subsurface tumor detection and margin assessment using human bone and STS xenografts in rodent models. Murine sarcoma xenograft models have facilitated our preclinical study of targeted (*i.e.*, ABY-029, a NIR epidermal growth factor receptor-targeted probe [59]) and untargeted (*i.e.*, ICG) fluorophores in human bone and STSs, demonstrating strong contrast in both STS and Ewing sarcoma. Heterogeneous staining of ABY-029 led us to attempt dual-agent staining with ICG administered 24 h before sarcoma removal in the “second window” imaging mode [60]. This evolution improved the overall contrast-to-variance ratio compared to either reporter alone. Research with multiple fluorophores in the same channel is warranted to further improve tumor-to-background contrast ratios. Furthermore, incorporation of multimodal imaging with LiDAR and conventional imaging-based navigation systems will likely improve overall accuracy.

Margin status is the ultimate determinant of local sarcoma management. Therefore, the use of NIR probes may be problematic given the deeper tissue penetration of longer optical wavelengths. We are now exploring additional fluorescence imaging of current probes using secondary excitation/emission spectra at lower (*i.e.*, blue) optical wavelengths that would prevent deeper tissue penetration and focus imaging on specimen surface tissues. Combinations of multi-spectral imaging, LiDAR, imaging-based navigation, and high-resolution CT scanning could provide improved margin status reporting, thereby increasing complete tumor removal and improving patient outcomes.

### Nerve Visualization

Iatrogenic injury is a common cause of surgical complications across all surgical specialties, accounting for nearly 600,000 nerve injuries annually in the United States alone [61]. Nerve injuries can result in chronic pain and reduced or lost motor function and/or sensation. While capable surgeons can identify and protect nerves in a normal surgical

field, patients involved in trauma and those with abnormal anatomy or prior surgery can make identification difficult. Laparoscopic surgeries, which rely on assumptions about normal anatomic planes rather than direct visualizations, are also at risk of iatrogenic injury [62]. With over 300 million surgeries being performed worldwide annually, the population that could benefit from measures to identify and protect nerves is difficult to identify [63].

Eight classes of nerve- or brain-specific fluorophores have been discovered, all of which fluoresce at visible wavelengths and struggle with nonspecific tissue uptake [21]. Increased specificity is important to improve the clinical effectiveness of any of these agents. Early preclinical trials involving synthetically modified, NIR, nerve-specific fluorophores have demonstrated improved specificity [21]. Additionally, imaging with a NIR (*i.e.*, longer wavelength) fluorophore reduces the effect of light scattering, which helps to improve the locational specificity of nerves imaged at depths up to ~3 mm. (An example of one such synthetically modified, NIR, nerve-specific fluorophore is demonstrated in Fig. 6.)

Future directions focus on identifying candidate fluorophores to evaluate nerve health, diagnose nerve injury, classify structural manifestation and degree of injury, and determine likelihood of recovery. Being able to identify nerves that may have been damaged in less visible ways (*e.g.*, stretched by a retractor, thermally damaged by hardening bone cement, crushed in the process of tying off vessels) would allow for more rapid and tangible repair or treatment. Better visualization and identification with the use of a fluorescent contrast agent would likely improve surgical outcomes and reduce the incidence of iatrogenic injury, especially in laparoscopic or trauma surgery.

## Challenges to Translation and Potential Solutions

### New Fluorophore Evaluation and Lead Agent Selection

The early successes of FGS guarantee future investigation, assuredly expanding the field of candidate fluorophores undergoing preclinical and clinical evaluation. This will lead to a demand for fluorophores with increased specificity and convenience to facilitate broader use [64, 65]. In this section, we discuss general strategies for streamlining fluorophore and imager development, with particular attention to resource-sensitive lead agent identification.

Achieving accurate, sensitive, and specific molecular-targeted fluorophores is the ultimate goal of FGS, particularly

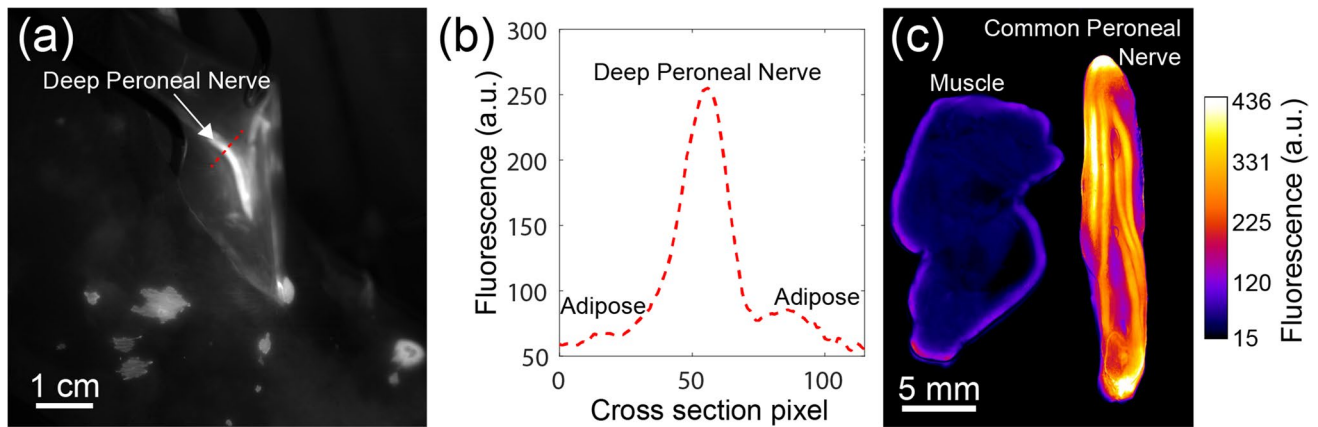


**Fig. 6** Representative fluorescence images demonstrating positive contrast using the nerve-specific, NIR fluorophore LGW16-03 in a human limb perfusion model. **a** Fluorescence highlights *in vivo* deep

peroneal nerve surrounded by adipose tissue; the intensity profile (red dashed line) is plotted in **b**. **c** *Ex vivo* tissues imaged highlight common peroneal nerve fluorescence relative to muscle tissue.

in surgical oncology where cancers are the target tissue [66]. One approach for creating fluorophores with a high degree of specificity is through creation of a library of derivatives from a known molecule which demonstrates a degree of desired specificity [21]. This library can then be tested to identify lead agents with the highest clinical promise. This, however, can be a daunting process, because fluorophore libraries may expand exponentially based on the number of molecular adjustments [67]. Several preclinical testing modalities exist to distill these libraries (*e.g.*, assays, gel modeling, and animal models), yet they lack performance analysis in human tissue.

Fluorophore performance metrics include safety and fluorescence contrast for the tissue or physiological phenomenon of interest. Often, fluorophore signal-to-background is the metric of interest when evaluating a potential lead agent. However, advancing new reporters to human trials, even via the FDA's phase 0/microdose pathway, requires significant resources and single-species pharmacokinetics and toxicity testing. Accurate lead agent selection for advancement to human trials is therefore of critical importance to avoid wasted time and capital resources [68]. Application of these agents to human tissue in a minimal risk environment could help to narrow the pool to a single agent and provide valuable data in the application process for FDA approval and for initial clinical trials.

In two ongoing, IRB-approved research studies, we use *ex vivo* human tissue that would otherwise be discarded for testing a preclinical nerve-specific fluorophore. In the first study, nerves and nerve-derived tumors are excised as part of standard-of-care treatment, and a nerve-specific, NIR fluorophore (a synthetic oxazine derivative known as LGW16-03, based on recent work by Wang et al. [21]) is topically applied. LGW16-03 is initially reconstituted to 1 mg/mL, and then 250 mL of fluorophore is diluted in 4750 mL of phosphate-buffered saline (PBS). Each tissue segment is then bathed for 5 min before three consecutive,

30-s washes in PBS. Snapshot images are then taken with the SPY Elite system, and fluorescence contrast measurements are compared to preclinical studies. This approach facilitates imaging of human nerve and nerve-derived tumors prior to in-human testing with no risk to patients beyond those associated with standard-of-care surgery. A total of 100 *ex vivo* specimens will be imaged in this study.

In the second study, LGW16-03 is administered to human tissues via systemic infusion. We obtain recently amputated human limbs and administer 10 mL of LGW16-03 via intraarterial perfusion after cannulating the dominant arterial vessel. (Again, LGW16-03 is initially reconstituted to 1 mg/mL, then 250 mL of fluorophore is diluted in 4750 mL of PBS prior to injection.) Perfusion is achieved via a cardiac bypass rotary pump in an approach that is similar to a previous limb perfusion model [69]. After perfusion, snapshot images of the nerve are taken *in vivo* with a wide-field imager (Solaris, PerkinElmer, Waltham, MA) after 10 min of perfusion and 20 min of subsequent washout with saline. The nerve is then excised and imaged *ex vivo* using a closed-field imager (Odyssey CLx, LI-COR Biosciences, Lincoln, NE). Both *in vivo* and *ex vivo* images show positive contrast between nerves and adjacent tissue (Fig. 6). A total of 10 perfused limbs will be imaged in this study. Preliminary fluorescence measurements of the deep peroneal nerve in a human limb perfusion model yield an *in vivo* nerve-to-adipose tissue intensity ratio of ~4.5 (Fig. 6a–b), and preliminary fluorescence measurements of the common peroneal nerve yield an *ex vivo* nerve-to-muscle tissue intensity ratio of ~7.5 (Fig. 6c).

There are limitations with this approach. First, amputations are relatively uncommon. Second, because normal human limbs are not amputated, most specimens have either chronic infection or vascular disease. Given the strong social benefits of organ procurement programs, in

the future there may be similar adoption of limb donation programs. Limb transplant programs are also increasing, indicating further need for evaluation of limb perfusion methods.

The use of human tissue in an *ex vivo* capacity is not novel; many studies involving transplant surgery currently make use of either discarded or nonviable human tissues [69–71]. Use of *ex vivo* human tissues provides an avenue to test and select lead agents in a safer and less expensive way than running several clinical trials with similar agents. For this study, only saline was used to perform systemic administration; however, future work could create a model which would fully sustain and perfuse a limb allowing for long-term administration and testing of fluorescent agents. This model would not only allow for nerve-specific fluorophores to be tested but also vascular-, biomarker-, and pathology-based imaging to be conducted by inducing specific environments within the limb. Research into improving the duration of limb viability already exists within the field of transplant surgery and provides the foundation to expand upon for the development of such a model [69].

### Tissue-Simulating Phantoms

Recent advances in imaging phantoms are paving the way for more quantitative fluorescence imaging techniques and inter-system characterization [72, 73], including fluorescent phantoms with tunable optical properties [74]. In addition to creating phantoms with specific fluorescence and optical properties, phantoms can be used as a testing platform of controlled circumstances in orthopaedic surgery. Our work focused on the development of gelatin-based, tissue-simulating phantoms [75]. These phantoms were composed of matrix, scattering, absorbing, and fluorescent materials, which were easily accessible and cost-effective [74, 76]. Various ratios of scattering and absorbing materials simulated optically different tissue types, such as muscle, adipose, and tumor tissues [77]. Molecules of specific interest were incorporated, such as fluorophores and contrast agents for CT and MRI [77, 78]. We subtly altered contrast agent concentrations in “tumor” inclusions and surrounding stroma. A trained surgeon then repeatedly resected the target inclusion based on different types/combinations of contrast, thereby facilitating evaluation of different imaging modalities for surgical guidance. The phantoms were highly turbid such that any simulated structures within the phantom were concealed when viewed under white light (Fig. 7). Due to reproducibility and the controlled surgical environment created, the gelatin phantoms represent a state-of-the-art methodology for comparing fluorescence imaging and conventional technologies for surgical navigation.

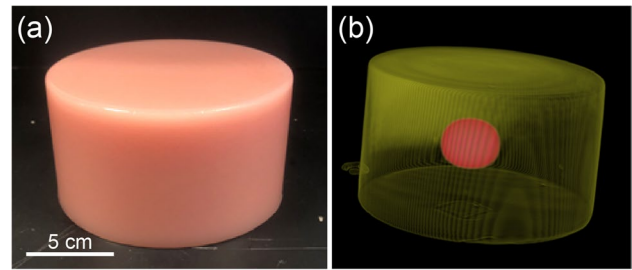


**Fig. 7** Gelatin-based, tissue-simulating phantom for assessing conventional medical imaging (*i.e.*, CT and MRI) and fluorescence imaging for surgical guidance. **a** White light image of a representative phantom. **b** Volumetric rendering of the same phantom showing tumor-simulating MRI contrast agent inclusion (red). Scale bar in **a** also applies to **b**.

### Fluorophore and Imager Evaluation—What Metrics Matter?

A key topic of discussion at recent international meetings has concerned the criteria by which new surgical guidance technologies are evaluated (*e.g.*, American Association of Physicists in Medicine Task Group 311 [79, 80] and the WMIS Optical Surgical Navigation Interest Group [81, 82]). Patient outcomes are clearly the gold standard for any novel clinical instrument. However, it has been suggested that this may be either too high a bar to clear or the wrong bar entirely. In some cases, FGS is not intended to change outcomes but to facilitate their realization more easily or quickly. For example, most surgeons will successfully identify the sciatic nerve during a revision hip replacement surgery. This may be done by dissecting the nerve from investing scar tissue, or alternatively, could be done with guidance from a NIR, nerve-specific fluorophore. The first approach is time-consuming but also time-tested; the second approach would be effectively instantaneous. In this scenario, patient outcomes may not change significantly between these approaches, but the latter approach may increase surgeon confidence, reduce operation times, and provide cost savings for patients and the healthcare system.

The use of qualitative, provider-completed surveys has been posited as an alternative to clinical outcomes in evaluating surgical guidance technologies. While qualitative endpoints are often scorned as soft metrics, it is worth noting that patient-reported outcome measures (PROMs) have become standard in evaluating patient outcomes in general [83]. In similar fashion, if surgeons are the end-users of a technology (*i.e.*, a fluorophore and/or imaging system) and believe that it provides increased confidence in their recognition of anatomical structures and surgical decision-making, these subjective conclusions should warrant similar attention to PROMs, even in the absence of statistically significant differences in occurrence of rare and catastrophic

events (e.g., sciatic nerve injury). Ultimately, the final gatekeeper of technology adoption are tax and insurance payers. Clear evidence of patient benefit with new technologies and techniques is an effective impetus for translation. Whether payers will be swayed by surgeon-reported qualitative endpoints, however, is yet to be tested.

## Conclusions

Despite rapid advancements in fluorescence guidance in several surgical fields, FGS applications in orthopaedic surgery are lagging. This review focused on three broad areas in which FGS may meaningfully improve patient care in orthopaedics: infection management, assessment of the regenerative capacity of tissues, and tissue identification. Continued research in these areas is needed to achieve translation, with particular attention paid to rigorous evaluation of new fluorophores and potential lead agents, the use of tissue-simulating fluorescent phantoms, and the establishment of meaningful metrics to evaluate new surgical guidance technologies in orthopaedic surgery.

**Author Contribution** All authors made substantial contributions to research design, or the acquisition, analysis, or interpretation of data and contributed to drafting the paper or revising it critically. All authors have read and approved the final submitted manuscript and agree to be accountable for all aspects of the work.

**Funding** Support for this article came from Hitchcock Foundation grant number 250–4141 and from NIH research grants K23EB026507, R01NS116994, and F31CA257340.

## Declarations

**Conflict of Interest** S. Streeter is a part-time employee of QUEL Imaging LLC, a Small Business Innovation Research-funded start-up that focuses on the commercialization of optical targets for fluorescence guided surgical systems. S. Gibbs is a co-founder and stockholder of Trace Biosciences, a start-up company focused on the development and clinical translation of nerve-specific probes for FGS. S. Gibbs also has three patents pending related to this work (US No. 62/711,465, US No. 62/729,932, and US No. 62/956,614). E. Henderson is an educational consultant for Stryker Orthopaedics. All other authors declare no competing interests.

## References

- Weissleder R, Mahmood U (2001) Molecular imaging. *Radiol* 219:316–333. <https://doi.org/10.1148/radiology.219.2.r01ma19316>
- van Leeuwen FWB, Hardwick JCH, van Erkel AR (2015) Luminescence-based imaging approaches in the field of interventional molecular imaging. *Radiology* 276:12–29. <https://doi.org/10.1148/radiol.2015132698>
- Paraboschi I, Farneti F, Jannello L, Manzoni G, Berrettini A, Mantica G (2022) Narrative review on applications of fluorescence guided surgery in adult and pediatric urology. *AME Med J* 7:15. <https://doi.org/10.21037/amj-20-194>
- Vahrmeijer AL, Hutteman M, van der Vorst JR et al (2013) Image-guided cancer surgery using near-infrared fluorescence. *Nat Rev Clin Oncol* 10:507–518. <https://doi.org/10.1038/nrclinonc.2013.123>
- Schouw HM, Huisman LA, Janssen YF et al (2021) Targeted optical fluorescence imaging: a meta-narrative review and future perspectives. *Eur J Nucl Med Mol Imaging* 48:4272–4292. <https://doi.org/10.1007/s00259-021-05504-y>
- Hadjipanayis CG, Widhalm G, Stummer W (2015) What is the surgical benefit of utilizing 5-aminolevulinic acid for fluorescence-guided surgery of malignant gliomas? *Neurosurg* 77:663–673. <https://doi.org/10.1227/NEU.0000000000000929>
- Cleary K, Peters TM (2010) Image-guided interventions: technology review and clinical applications. *Annu Rev Biomed Eng* 12:119–142. <https://doi.org/10.1146/annurev-bioeng-070909-105249>
- Park HY, Zoller SD, Hegde V et al (2021) Comparison of two fluorescent probes in preclinical non-invasive imaging and image-guided debridement surgery of Staphylococcal biofilm implant infections. *Sci Rep* 11:1622. <https://doi.org/10.1038/s41598-020-78362-7>
- Garcia D, Gardezi M, Suliman Y et al (2021) Fluorescent-conjugated antibodies as rapid ex vivo markers for bacterial presence on orthopedic surgical explants and synovium: a pilot study. *J Orthop Res* 39:299–307. <https://doi.org/10.1002/jor.24924>
- Green JM III, Sabino J, Fleming M, Valerio I (2015) Intraoperative fluorescence angiography: a review of applications and outcomes in war-related trauma. *Mil Med* 180:37–43. <https://doi.org/10.7205/MILMED-D-14-00632>
- Gitajn IL, Elliott JT, Gunn JR et al (2020) Evaluation of bone perfusion during open orthopedic surgery using quantitative dynamic contrast-enhanced fluorescence imaging. *Biomed Opt Express* 11:6458–6469. <https://doi.org/10.1364/BOE.399587>
- Kim SH, Cho W-S, Joung H-Y et al (2017) Perfusion of the rotator cuff tendon according to the repair configuration using an indocyanine green fluorescence arthroscope: a preliminary report. *Am J Sports Med* 45:659–665. <https://doi.org/10.1177/0363546516669778>
- Doi N, Izaki T, Miyake S et al (2019) Intraoperative evaluation of blood flow for soft tissues in orthopaedic surgery using indocyanine green fluorescence angiography: A pilot study. *Bone Joint Res* 8:118–125. <https://doi.org/10.1302/2046-3758.83.BJR-2018-0151.R1>
- Samkoe KS, Bates BD, Elliott JT et al (2018) Application of fluorescence-guided surgery to subsurface cancers requiring wide local excision: literature review and novel developments toward indirect visualization. *Cancer Control* 25:1073274817752332. <https://doi.org/10.1177/1073274817752332>
- Bosma SE, van Driel PB, Hogendoorn PC et al (2018) Introducing fluorescence guided surgery into orthopedic oncology: a systematic review of candidate protein targets for Ewing sarcoma. *J Surg Oncol* 118:906–914. <https://doi.org/10.1002/jso.25224>
- Samkoe KS, Sardar HS, Bates BD et al (2019) Preclinical imaging of epidermal growth factor receptor with ABY-029 in soft-tissue sarcoma for fluorescence-guided surgery and tumor detection. *J Surg Oncol* 119:1077–1086. <https://doi.org/10.1002/jso.25468>
- Guder WK, Hartmann W, Buhles C et al (2022) 5-ALA-mediated fluorescence of musculoskeletal tumors in a chick chorio-allantoic membrane model: preclinical in vivo qualification analysis as a fluorescence-guided surgery agent in Orthopedic Oncology. *J Orthop Surg Res* 17:34. <https://doi.org/10.1186/s13018-022-02931-x>
- Rijs Z, Jeremiasse B, Shifai N, et al (2021) Introducing fluorescence-guided surgery for pediatric Ewing, osteo-, and

- rhabdomyosarcomas: a literature review. *Biomedicines* 9. <https://doi.org/10.3390/biomedicines9101388>
19. Gibbs-Strauss SL, Nasr KA, Fish KM et al (2010) (2011) Nerve-highlighting fluorescent contrast agents for image-guided surgery. *Mol Imaging* 10(7290):00026. <https://doi.org/10.2310/7290.2010.00026>
  20. Chen Y, Zhang H, Lei Z, Zhang F (2020) Recent advances in intraoperative nerve bioimaging: fluorescence-guided surgery for nerve preservation. *Small Struct* 1:2000036. <https://doi.org/10.1002/ssstr.202000036>
  21. Wang Lei G, Barth Connor W, Kitts Catherine H et al (2020) Near-infrared nerve-binding fluorophores for buried nerve tissue imaging. *Sci Transl Med* 12:eaay0712. <https://doi.org/10.1126/scitranslmed.aay0712>
  22. Barth CW, Shah VM, Wang LG et al (2022) A clinically relevant formulation for direct administration of nerve specific fluorophores to mitigate iatrogenic nerve injury. *Biomaterials* 284:121490. <https://doi.org/10.1016/j.biomaterials.2022.121490>
  23. Imaging of Infections (IOI) Interest Group | World Molecular Imaging Society. <https://www.wmis.org/wmis-interest-groups-main/imaging-of-infections-interest-group-main/>. Accessed 22 Oct 2022
  24. Gordon O, Ruiz-Bedoya Camilo A, Ordonez Alvaro A et al (2019) Molecular imaging: a novel tool to visualize pathogenesis of infections in situ. *mBio* 10:00317–19. <https://doi.org/10.1128/mBio.00317-19>
  25. Gordon O, Lee DE, Liu B et al (2021) Dynamic PET-facilitated modeling and high-dose rifampin regimens for *Staphylococcus aureus* orthopedic implant-associated infections. *Sci Transl Med* 13:l6851. <https://doi.org/10.1126/scitranslmed.abl6851>
  26. Schoenmakers JWA, Heuker M, López-Álvarez M et al (2021) Image-guided in situ detection of bacterial biofilms in a human prosthetic knee infection model: a feasibility study for clinical diagnosis of prosthetic joint infections. *Eur J Nucl Med Mol Imaging* 48:757–767. <https://doi.org/10.1007/s00259-020-04982-w>
  27. Turecki MB, Taljanovic MS, Stubbs AY et al (2010) Imaging of musculoskeletal soft tissue infections. *Skeletal Radiol* 39:957–971. <https://doi.org/10.1007/s00256-009-0780-0>
  28. Beristain-Covarrubias N, Perez-Toledo M, Thomas MR et al (2019) Understanding infection-induced thrombosis: lessons learned from animal models. *Front Immunol* 10:2569. <https://doi.org/10.3389/fimmu.2019.02569>
  29. Wong C-H, Khin L-W, Heng K-S et al (2004) The LRINEC (Laboratory Risk Indicator for Necrotizing Fasciitis) score: a tool for distinguishing necrotizing fasciitis from other soft tissue infections. *Crit Care Med* 32:1535–1541. <https://doi.org/10.1097/01.ccm.0000129486.35458.7d>
  30. McHenry CR, Piotrowski JJ, Petrinic D, Malangoni MA (1995) Determinants of mortality for necrotizing soft-tissue infections. *Ann Surg* 221:558–565. <https://doi.org/10.1097/00000658-199505000-00013>
  31. Stevens DL, Bisno AL, Chambers HF et al (2014) Practice guidelines for the diagnosis and management of skin and soft tissue infections: 2014 update by the Infectious Diseases Society of America. *Clin Infect Dis* 59:e10–e52. <https://doi.org/10.1093/cid/ciu296>
  32. Stevens DL, Bryant AE (2017) Necrotizing soft-tissue infections. *N Engl J Med* 377:2253–2265. <https://doi.org/10.1056/NEJMa1600673>
  33. Wong C-H, Chang H-C, Pasupathy S et al (2003) Necrotizing fasciitis: clinical presentation, microbiology, and determinants of mortality. *J Bone Joint Surg Am* 85:1454–1460
  34. Pogue BW, Rosenthal EL (2021) Review of successful pathways for regulatory approvals in open-field fluorescence-guided surgery. *J Biomed Opt* 26:030901. <https://doi.org/10.1117/1.JBO.26.3.030901>
  35. Logerstedt DS, Snyder-Mackler L, Ritter RC, Axe MJ (2010) Knee pain and mobility impairments: meniscal and articular cartilage lesions. *J Orthop Sports Phys Ther* 40:A1–A35. <https://doi.org/10.2519/jospt.2010.0304>
  36. Bilgen B, Jayasuriya CT, Owens BD (2018) Current concepts in meniscus tissue engineering and repair. *Adv Healthc Mater* 7:e1701407. <https://doi.org/10.1002/adhm.201701407>
  37. Karia M, Ghaly Y, Al-Hadithy N et al (2019) Current concepts in the techniques, indications and outcomes of meniscal repairs. *Eur J Orthop Surg Traumatol* 29:509–520. <https://doi.org/10.1007/s00590-018-2317-5>
  38. Lohmander LS, Englund PM, Dahl LL, Roos EM (2007) The long-term consequence of anterior cruciate ligament and meniscus injuries: osteoarthritis. *Am J Sports Med* 35:1756–1769. <https://doi.org/10.1177/0363546507307396>
  39. Williams LB, Adesida AB (2018) Angiogenic approaches to meniscal healing. *Injury* 49:467–472. <https://doi.org/10.1016/j.injury.2018.01.028>
  40. Cinque ME, DePhillipo NN, Moatshe G et al (2019) Clinical outcomes of inside-out meniscal repair according to anatomic zone of the meniscal tear. *Orthop J Sports Med* 7:2325967119860806. <https://doi.org/10.1177/2325967119860806>
  41. Bray RC, Smith JA, Eng MK et al (2001) Vascular response of the meniscus to injury: effects of immobilization. *J Orthop Res* 19:384–390. [https://doi.org/10.1016/S0736-0266\(00\)00037-1](https://doi.org/10.1016/S0736-0266(00)00037-1)
  42. Bryceland JK, Powell AJ, Nunn T (2017) Knee menisci: structure, function, and management of pathology. *CARTILAGE* 8:99–104. <https://doi.org/10.1177/1947603516654945>
  43. Lapner P, Pollock JW, Zhang T et al (2020) A randomized controlled trial comparing subscapularis tenotomy with peel in anatomic shoulder arthroplasty. *J Shoulder Elbow Surg* 29:225–234. <https://doi.org/10.1016/j.jse.2019.09.028>
  44. Buckley T, Miller R, Nicandri G et al (2014) Analysis of subscapularis integrity and function after lesser tuberosity osteotomy versus subscapularis tenotomy in total shoulder arthroplasty using ultrasound and validated clinical outcome measures. *J Shoulder Elbow Surg* 23:1309–1317. <https://doi.org/10.1016/j.jse.2013.12.009>
  45. Shields E, Ho A, Wiater JM (2017) Management of the subscapularis tendon during total shoulder arthroplasty. *J Shoulder Elbow Surg* 26:723–731. <https://doi.org/10.1016/j.jse.2016.11.006>
  46. McCarthy I (2006) The physiology of bone blood flow: a review. *J Bone Joint Surg Am* 88(3):4–9. <https://doi.org/10.2106/JBJS.F.00890>
  47. Marenzana M, Arnett TR (2013) The key role of the blood supply to bone. *Bone Res* 1:203–215. <https://doi.org/10.4248/BR201303001>
  48. Buckley RE, Moran CG, Apivatthakakul T (2022) *AO Principles of Fracture Management: Vol. 1: Principles, Vol. 2: Specific fractures*, 3rd ed. Thieme Publishing Group, Stuttgart, Germany
  49. Angelini A, Battiato C (2015) Past and present of the use of cerclage wires in orthopedics. *Eur J Orthop Surg Traumatol* 25:623–635. <https://doi.org/10.1007/s00590-014-1520-2>
  50. Agarwala S, Menon A, Chaudhari S (2017) Cerclage wiring as an adjunct for the treatment of femur fractures: series of 11 cases. *J Orthop Case Rep* 7:39–43. <https://doi.org/10.13107/jocr.2250-0685.842>
  51. Perren SM, Fernandez Dell'oca A, Regazzoni P (2015) Fracture fixation using cerclage, research applied to surgery. *Acta Chir Orthop Traumatol Cech* 82:389–397
  52. Karakoyun O, Sahin E, Erol MF et al (2016) Effect of cable cerclage on regional blood circulation in rabbits: a scintigraphic study. *J Orthop Surg (Hong Kong)* 24:367–369. <https://doi.org/10.1177/1602400319>

53. Elliott JT, Addante RR, Slobogean GP et al (2020) Intraoperative fluorescence perfusion assessment should be corrected by a measured subject-specific arterial input function. *J Biomed Opt* 25:1–13. <https://doi.org/10.1117/1.JBO.25.6.066002>
54. Wirth D, Byrd B, Meng B et al (2021) Hyperspectral imaging and spectral unmixing for improving whole-body fluorescence cryo-imaging. *Biomed Opt Express* 12:395–408. <https://doi.org/10.1364/BOE.410810>
55. Dormans JP, Hanna BG, Johnston DR, Khurana JS (2004) Surgical treatment and recurrence rate of aneurysmal bone cysts in children. *Clin Orthop Relat Res* 421:205–211. <https://doi.org/10.1097/01.blo.0000126336.46604.e1>
56. Arbeitsgemeinschaft Knochentumoren, Becker WT, Dohle J, Bernd L, Braun A, Cserhati M, Enderle A, Hovy L, Matejovsky Z, Szendroi M, Trieb K, Tunn PU (2008) Local recurrence of giant cell tumor of bone after intralesional treatment with and without adjuvant therapy. *J Bone Joint Surg Am* 90(5):1060–7. <https://doi.org/10.2106/JBJS.D.02771>
57. Trautmann F, Schuler M, Schmitt J (2015) Burden of soft-tissue and bone sarcoma in routine care: estimation of incidence, prevalence and survival for health services research. *Cancer Epidemiol* 39:440–446. <https://doi.org/10.1016/j.canep.2015.03.002>
58. Pisters PW, Leung DH, Woodruff J et al (1996) Analysis of prognostic factors in 1,041 patients with localized soft tissue sarcomas of the extremities. *J Clin Oncol* 14:1679–1689. <https://doi.org/10.1200/JCO.1996.14.5.1679>
59. Samkoe KS, Gunn JR, Marra K et al (2017) Toxicity and pharmacokinetic profile for single-dose injection of ABY-029: a fluorescent anti-EGFR synthetic affibody molecule for human use. *Mol Imaging Biol* 19:512–521. <https://doi.org/10.1007/s11307-016-1033-y>
60. Newton AD, Predina JD, Corbett CJ et al (2019) Optimization of second window indocyanine green for intraoperative near-infrared imaging of thoracic malignancy. *J Am Coll Surg* 228:188–197. <https://doi.org/10.1016/j.jamcollsurg.2018.11.003>
61. Burke S, Shorten GD (2009) When pain after surgery doesn't go away.... *Biochem Soc Trans* 37:318–322. <https://doi.org/10.1042/BST0370318>
62. Palaniappa NC, Telem DA, Ranasinghe NE, Divino CM (2012) Incidence of iatrogenic ureteral injury after laparoscopic colectomy. *Arch Surg* 147:267–271. <https://doi.org/10.1001/archsurg.2011.2029>
63. Dobson GP (2020) Trauma of major surgery: a global problem that is not going away. *Int J Surg* 81:47–54. <https://doi.org/10.1016/j.ijss.2020.07.017>
64. DSouza AV, Lin H, Henderson ER et al (2016) Review of fluorescence guided surgery systems: identification of key performance capabilities beyond indocyanine green imaging. *J Biomed Opt* 21:80901. <https://doi.org/10.1117/1.JBO.21.8.080901>
65. Walsh EM, Cole D, Tipirneni KE et al (2019) Fluorescence imaging of nerves during surgery. *Ann Surg* 270:69–76. <https://doi.org/10.1097/SLA.0000000000003130>
66. Gibbs SL (2012) Near infrared fluorescence for image-guided surgery. *Quant Imaging Med Surg* 2:177–187. <https://doi.org/10.3978/j.issn.2223-4292.2012.09.04>
67. Park MH, Hyun H, Ashitate Y et al (2014) Prototype nerve-specific near-infrared fluorophores. *Theranostics* 4:823–833. <https://doi.org/10.7150/thno.8696>
68. Atallah I, Milet C, Coll J-L et al (2015) Role of near-infrared fluorescence imaging in head and neck cancer surgery: from animal models to humans. *Eur Arch Otorhinolaryngol* 272:2593–2600. <https://doi.org/10.1007/s00405-014-3224-y>
69. Werner NL, Alghanem F, Rakestraw SL et al (2017) Ex situ perfusion of human limb allografts for 24 hours. *Transplantation* 101(3):e68–e74
70. Cypel M, Yeung JC, Liu M et al (2011) Normothermic ex vivo lung perfusion in clinical lung transplantation. *N Engl J Med* 364:1431–1440. <https://doi.org/10.1056/NEJMoa1014597>
71. Lam VWT, Laurence JM, Richardson AJ et al (2013) Hypothermic machine perfusion in deceased donor kidney transplantation: a systematic review. *J Surg Res* 180:176–182. <https://doi.org/10.1016/j.jss.2012.10.055>
72. Gorpas D, Koch M, Anastasopoulou M et al (2017) Benchmarking of fluorescence cameras through the use of a composite phantom. *J Biomed Opt* 22:1–12. <https://doi.org/10.1117/1.JBO.22.1.016009>
73. Liu Y, Ghassemi P, Depkon A et al (2018) Biomimetic 3D-printed neurovascular phantoms for near-infrared fluorescence imaging. *Biomed Opt Express* 9:2810–2824. <https://doi.org/10.1364/BOE.9.002810>
74. Ruiz AJ, Garg S, Streeter SS et al (2021) 3D printing fluorescent material with tunable optical properties. *Sci Rep* 11:17135. <https://doi.org/10.1038/s41598-021-96496-0>
75. Henderson ER, Hebert KA, Werth PM, et al (2022) Fluorescence guidance improves the accuracy of radiological imaging-guided surgical navigation. *J Surg Oncol*. <https://doi.org/10.1002/jso.27128>
76. Pogue BW, Patterson MS (2006) Review of tissue simulating phantoms for optical spectroscopy, imaging and dosimetry. *J Biomed Opt* 11:1–16. <https://doi.org/10.1117/1.2335429>
77. Huber JS, Peng Q, Moses WW (2009) Multi-modality phantom development. *IEEE Trans Nucl Sci* 56:2722–2727. <https://doi.org/10.1109/TNS.2009.2028073>
78. Samkoe KS, Bates BD, Tselepidakis NN et al (2017) Development and evaluation of a connective tissue phantom model for subsurface visualization of cancers requiring wide local excision. *J Biomed Opt* 22:1–12. <https://doi.org/10.1117/1.JBO.22.12.121613>
79. Pogue BW, Zhu TC, Ntziachristos V et al (2018) Fluorescence-guided surgery and intervention — an AAPM emerging technology blue paper. *Med Phys* 45:2681–2688. <https://doi.org/10.1002/mp.12909>
80. AAPM Committee Tree - Task Group No. 311 - Guidance for Technical Performance Evaluation for Fluorescence Guided Surgery Systems (TG311). [https://www.aapm.org/org/structure/?committee\\_code=TG311](https://www.aapm.org/org/structure/?committee_code=TG311). Accessed 21 Oct 2022
81. Optical Surgical Navigation (OSN/ASIGS) Interest Group | World Molecular Imaging Society. <https://www.wmis.org/wmis-interest-groups-main/osnig-main/>. Accessed 21 Oct 2022
82. Rosenthal EL, Warram JM, de Boer E et al (2016) Successful translation of fluorescence navigation during oncologic surgery: a consensus report. *J Nucl Med* 57:144. <https://doi.org/10.2967/jnumed.115.158915>
83. Churrua K, Pomare C, Ellis LA et al (2021) Patient-reported outcome measures (PROMs): a review of generic and condition-specific measures and a discussion of trends and issues. *Health Expect* 24:1015–1024. <https://doi.org/10.1111/hex.13254>

**Publisher's Note** Springer Nature remains neutral with regard to jurisdictional claims in published maps and institutional affiliations.

Springer Nature or its licensor (e.g. a society or other partner) holds exclusive rights to this article under a publishing agreement with the author(s) or other rightsholder(s); author self-archiving of the accepted manuscript version of this article is solely governed by the terms of such publishing agreement and applicable law.